



On measuring the temperature coefficient of resistivity and the thermal expansion coefficient of conductive thin films

Gerhard Fischerauer 

Chair of Measurement and Control Systems, Universität Bayreuth, Universitätsstr. 30, 95447 Bayreuth, Germany



ARTICLE INFO

Keywords:

Thin films
Temperature coefficient of resistivity
Thermal expansion coefficient
Electrical measurement
Distinguishability

ABSTRACT

We analyze the details of extracting the temperature coefficient of resistivity and the thermal expansion coefficient of thin-film materials from the measured temperature coefficient of resistance of thin-film resistors on supporting substrates. It is shown that this requires two straining experiments, one thermal experiment, and the ability to deposit identical films on two different substrates with known properties. An analysis of experimental data from the literature, which includes the application of accepted rules from the Guide to the Expression of Uncertainty in Measurement (GUM), reveals that the violation of the stated requirements usually leads to inconsistent or arbitrary results.

1. Introduction

It is well known that thin films are characterized by effective material parameters that are different from the corresponding bulk values. The difference is caused on the one hand by the fact that surface effects play a greater role in thin films than in bulk materials. For example, aluminum always forms a layer of aluminum nitride (Al_2O_3) on its surface, and this layer contributes the more to the effective characteristics of an aluminum film, the thinner the film is.

On the other hand, the characteristics of a film are influenced by its morphology which depends on the details of the processes that have been used to deposit it on a supporting substrate. For example, the mass density of silicon carbide thin films deposited by plasma-enhanced chemical vapor deposition (PECVD) on GaAs is around $2,100 \text{ kg/m}^3$, depending somewhat on the film thickness [1,2], which is 33 % lower than the bulk value of $3,128 \text{ kg/m}^3$ [3]. Young's modulus and Poisson's ratio for the same films are around 140 GPa and 0.3, respectively [1,2]. The corresponding bulk values amount to 400 GPa (185 % above the thin-film value) [3, Table 223, p. 763] and 0.2 (33 % below the thin-film value) [3, Table 249, p. 823].

The substantial differences between bulk and thin-film material parameters explain the need for direct measurements on thin films. We are interested in the temperature dependence of the resistance of thin-film samples and in shedding light on the factors that contribute to this temperature dependence. The resistance of a thin-film device is an integral parameter which depends on both material properties (resistivity of the thin-film material) and geometry (length, width and height of the

film). Both the material properties and the geometry are functions of temperature. The situation is complicated by the fact that the geometry of the supporting substrate also depends on temperature. Measurements on film/substrate geometries must be interpreted carefully. It is easy to misinterpret effects as caused by the film when in reality they are consequences of the film/substrate coupling. It is even easier to obtain wrong numbers for thin-film material parameters such as the resistivity by such a misinterpretation of measured data.

For thin metal wires, it has been shown that neglecting thermal expansion effects leads to significant errors, so significant indeed that even the sign of the temperature coefficient of resistivity can be wrong when the coefficient is derived from measured resistances in this manner [4]. The literature on thin films provides numerous examples with material data (resistivities and temperature coefficients of resistivity) that have been derived from resistance measurements without taking into account thermal expansion effects. It is the aim of this contribution to provide a framework for correct data interpretation and to show to what extent the numerical values change when this approach is followed.

It is not our goal to trace back the measured material parameters to more fundamental parameters such as film morphology, mean free path length of electrons, specularity parameter (probability of an electron to be specularly reflected from the surface), etc. It is true that physical theories such as the well-known Fuchs-Sondheimer model [5] or the Mayadas-Shatzkes model [6,7] for the resistivity of thin films allow one to predict measurable quantities and thus to judge the plausibility or quality of measurement data. It is also true, however, that such theory-based approaches can fail dramatically when the assumptions

E-mail address: mrt@uni-bayreuth.de.

behind the theory are not satisfied. Sambles opined >40 years ago that the area of thin-film research in general and resistivity measurements in particular would “be cluttered further with trivial and almost worthless experimental data” unless experimenters paid close attention to a number of points that were often overlooked [8]. This verdict is as valid today as it was back then. As Thompson has shown only a few years later [9,10], the situation may improve if one combines theory-based approaches with an appropriate processing of experimental data. But the situation does not necessarily have to improve as processing errors can lead to erroneous thin-film parameters even though the underlying physical theory is correct. Common errors include assumptions regarding the bulk values of material parameters, comparison of samples with different thin-film structures, and failure to consider outcome quality measures [9]. Although we do not strive to compute resistivity and its dependence on temperature from more basic physical quantities by way of physical theory, the mentioned data processing errors can also occur when measuring the thin-film resistivity directly and will therefore be included in our treatment.

2. Problem analysis and model development

2.1. Geometries with homogeneous current density

Let us consider a thin-film resistor made of an isotropic material with resistivity ρ_f , the index “f” being used to indicate a material property of the film. The current density inside the film shall be homogeneous. When the dimensions of the resistor are ℓ (length, aligned with the x-axis of a Cartesian coordinate system), w (width, in y-direction), and h (height, in z-direction), its resistance is given by

$$R = \rho_f \frac{\ell}{wh}. \quad (1)$$

This resistance varies when the quantities on the right-hand side vary. Differentiating by parts or looking into the literature—see, e. g., [11, Eq. (2)] or [12, Eq. (4)]—shows that

$$\frac{\Delta R}{R} = \frac{\Delta \rho_f}{\rho_f} + \frac{\Delta \ell}{\ell} - \frac{\Delta w}{w} - \frac{\Delta h}{h} = \frac{\Delta \rho_f}{\rho_f} + \varepsilon_{xf} - \varepsilon_{yf} - \varepsilon_{zf}. \quad (2)$$

Here, ε_{xf} , ε_{yf} and ε_{zf} are the relative length changes, or strains, of the film in the x-, y- and z-directions, respectively. Eq. (2) is a quantitative way of stating that changes in the device parameter “resistance” are caused by changes in the material parameter “resistivity” or changes in the geometry (or both).

Strains are caused by mechanical stresses or by temperature changes (thermal expansion). By ignoring shear components in Hooke’s law, one obtains [13, Eq. (3)]

$$\begin{pmatrix} \varepsilon_{xf} \\ \varepsilon_{yf} \\ \varepsilon_{zf} \end{pmatrix} = \frac{1}{E_f} \begin{pmatrix} 1 & -\mu_f & -\mu_f \\ -\mu_f & 1 & -\mu_f \\ -\mu_f & -\mu_f & 1 \end{pmatrix} \begin{pmatrix} \sigma_{xf} \\ \sigma_{yf} \\ \sigma_{zf} \end{pmatrix} + \begin{pmatrix} 1 \\ 1 \\ 1 \end{pmatrix} \alpha_{sf} \Delta T \quad (3)$$

where E_f , μ_f and α_{sf} respectively denote Young’s modulus, Poisson’s ratio, and the thermal expansion coefficient of the thin-film material. σ_{xf} , σ_{yf} and σ_{zf} are the normal stress components in the film in the x-, y-, and z-directions, respectively (in compressed index notation). ΔT is the difference between the instantaneous temperature and the reference temperature at which the dimensions of the resistor are considered as unstrained.

In general, the fractional change in resistivity, too, will depend on mechanical stresses and on temperature:

$$\frac{\Delta \rho_f}{\rho_f} = (\pi_{xxf} \quad \pi_{xyf} \quad \pi_{xzf}) \begin{pmatrix} \sigma_{xf} \\ \sigma_{yf} \\ \sigma_{zf} \end{pmatrix} + \alpha_{sf} \Delta T \quad (4)$$

where the π_{ijf} are components of the piezoresistivity tensor (in com-

pressed index notation) and α_{sf} is the linear temperature coefficient of resistivity.

Eqs. (2), (3) and (4) together describe how the resistance changes when the resistor is mechanically stressed or subjected to temperature variations. We proceed by considering two special cases.

2.1.1. Thin films with uniaxial stress

Let a thin-film resistor be subjected to uniaxial stress in the x-direction ($\sigma_{xf} \neq 0$, $\sigma_{yf} = \sigma_{zf} = 0$) and to temperature effects ($\Delta T \neq 0$). Inserting the stress conditions into Eqs. (3) and (4) and combining the resulting equations with Eq. (2) yields:

$$\frac{\Delta R}{R} = \frac{1}{E_f} K_{GF} \sigma_{xf} + (\alpha_{sf} - \alpha_{sf}) \Delta T \quad (5)$$

with the “gauge factor”

$$K_{GF} = \pi_{xxf} E_f + 1 + 2\mu_f. \quad (6)$$

We conclude the following:

(a) For a purely mechanical experiment with $\Delta T = 0$, Eq. (5) reduces to

$$\frac{\Delta R}{R} = \frac{1}{E_f} K_{GF} \sigma_{xf} = K_{GF} \varepsilon_{xf}. \quad (7)$$

This shows that the gauge factor K_{GF} can be determined by straining the resistor along its length direction and measuring the resulting resistance change.

(b) Without external forces acting on the thin film, $\sigma_{xf} = 0$, Eq. (5) reduces to

$$\frac{\Delta R}{R} = (\alpha_{sf} - \alpha_{sf}) \Delta T =: \alpha_R \Delta T. \quad (8)$$

Obviously, one can measure the overall temperature coefficient of resistance, α_R , but not the individual contributions of the material parameters α_{sf} and α_{sf} of the film.

Note that an experiment of type (b) usually requires a suspended thin film but is hardly conceivable for a thin film deposited on a substrate. The conditions $\sigma_{xf} = 0$ and $\sigma_{yf} = 0$ exclude any thermal expansion mismatch between the film and the substrate. Generally, the film will be strained by the substrate at temperatures other than room temperature when the system was stress-free at room temperature (so-called misfit strains).

2.1.2. Supported thin films with biaxial stress due to thermal expansion

A thin film deposited on a substrate does not exhibit any out-of-plane stress unless such stress is intentionally applied. We do not consider such intentional stressing and therefore set $\sigma_{zf} = 0$. In the xy-plane, however, the film cannot move freely as the coupling to the substrate introduces constraints. We assume isotropic biaxial stress: $\sigma_{xf} = \sigma_{yf}$. Eqs. (3) and (4) then become

$$\begin{pmatrix} \varepsilon_{xf} \\ \varepsilon_{yf} \\ \varepsilon_{zf} \end{pmatrix} = \frac{1}{E_f} \begin{pmatrix} 1 - \mu_f \\ 1 - \mu_f \\ -2\mu_f \end{pmatrix} \sigma_{xf} + \begin{pmatrix} 1 \\ 1 \\ 1 \end{pmatrix} \alpha_{sf} \Delta T \quad (9)$$

and

$$\frac{\Delta \rho_f}{\rho_f} = (\pi_{xxf} + \pi_{yxf}) \sigma_{xf} + \alpha_{sf} \Delta T. \quad (10)$$

There is some disagreement in the literature on how the (average)

stress σ_{xf} in a layer supported by a substrate should be computed. Under the assumption of perfect bonding between film and substrate (no-slip condition), any deformation of the substrate also leads to a deformation of the thin film. An often-cited equation due to Stoney is [14, Eq. (1) Eq. (1)]

$$\sigma_{xf} = \frac{1}{6} \frac{E_s}{1 - \mu_s} \frac{h_s}{hr} \quad (11)$$

where E_s and μ_s are Young's modulus and Poisson's ratio of the substrate material, respectively. Furthermore, h_s denotes the substrate height and r is the radius of curvature of the coated substrate at a temperature difference ΔT with respect to the temperature at which the substrate is unstressed and therefore flat ($r \rightarrow \infty$).

In practice, it may be difficult to mechanically stress a supported thin film in a controlled manner. When the thermal expansion coefficients of the film and substrate materials differ, one can exploit the thermal-misfit stress created by temperature increases. This has the disadvantage that the influences of piezoresistivity and thermal expansion on the device resistance now act together, but we will see below that they can be separated by performing three independent experiments.

A common expression for the stress in a supported thin film caused by thermal expansion is [14, Eq. (2)]

$$\sigma_{xf} = \frac{E_f}{1 - \mu_f} (\alpha_{s1} - \alpha_{f1}) \Delta T. \quad (12)$$

This expression assumes a rigid, incompressible, inflexible substrate [14]. It does not account for the equilibria of the film and substrate stresses on the one hand and the bending moments on the other hand. Such stresses and moments necessarily occur with temperature changes when film and substrate have different thermal expansion coefficients. As pointed out by Chiu [14], combining Eqs. (11) and (12) is equivalent to treating the substrate as simultaneously flexible and inflexible. This, although found in the literature, is inconsistent and leads to wrong conclusions.

The correct equation, which takes the mentioned equilibria into account, is lengthy [14, Eq. (B-5)]. But for thin films with a large thickness ratio h_s/h —on the order of $(100 \mu\text{m})/(100 \text{ nm}) = 1000$ —and when the ratio of the elastic moduli, E_s/E_f , is not exceedingly large, the film stress σ_{xf} can be approximated very well by its saturation value

$$\sigma_{xf} = E_f (\alpha_{s1} - \alpha_{f1}) \Delta T. \quad (13)$$

This equation considers the coated system as a linearly elastic framework whereas, as mentioned, Eq. (12) treats the substrate as rigid. Eqs. (2), (9), (10), (13) together yield

$$\frac{\Delta R}{R} = (K'_{GF} (\alpha_{s1} - \alpha_{f1}) + \alpha_{pf} - \alpha_{f1}) \Delta T =: \alpha'_R \Delta T \quad (14)$$

with the gauge factor

$$K'_{GF} = (\pi_{xxf} + \pi_{xyf}) E_f + 2\mu_f \quad (= K_{GF} - 1 + \pi_{xyf} E_f). \quad (15)$$

Eq. (14) degenerates to Eq. (8) for $\alpha_{f1} = \alpha_{s1}$ (thermal expansion match between thin film and substrate). This is to be expected as the substrate does not exert any forces on a film when the film-substrate system expands uniformly. In any other case, the gauge factor K'_{GF} and the temperature coefficient of resistance α'_R valid for a resistor based on a supported thin film differ from the corresponding values K_{GF} and α_R of the suspended thin film. K'_{GF} describes a biaxial-stress case whereas K_{GF} is valid for uniaxial stress. In the absence of a transverse piezoresistive effect, i.e., when $\pi_{xyf} = 0$, $K'_{GF} = K_{GF} - 1$; for isotropy, i.e., when $\pi_{xyf} = \pi_{xxf}$, $K'_{GF} = 2 \cdot (K_{GF} - 1 - \mu_f)$. Some caution must be exercised to make sure that such relations hold. As noted by Rosenberg [15], “simple relations which often appear in the literature should be dealt with cautiously because they usually treat the resistivity of metals as a scalar, thus eliminating one of the piezoresistance coefficients.”

By Eq. (14), α'_R can be determined by heating the film-substrate system and measuring the resistances at different temperatures. The same is not true for α_{pf} . A thermal cycling experiment only yields α'_R , i.e., a weighted combination of the coefficients α_{pf} and α_{f1} (material properties of the film) and α_{s1} (a material property of the substrate). α_{s1} may be known for common substrates such as glass, and the gauge factor K'_{GF} may be determined by mechanically straining the resistor. But even when α_{s1} and K'_{GF} are known, one cannot quantify the individual contributions of α_{pf} and α_{f1} towards α'_R . All one can infer is the numerical value of the linear combination

$$\alpha_{pf} - (1 + K'_{GF}) \alpha_{f1} = \alpha'_R - K'_{GF} \alpha_{s1}. \quad (16)$$

If it is possible to deposit films with identical material parameters on two different substrates, one can use Eq. (14) twice and subtract them from one another. This leads to

$$K'_{GF} = \frac{\alpha'_{R1} - \alpha'_{R2}}{\alpha_{s1} - \alpha_{s2}}. \quad (17)$$

Of course, given the importance of the substrate surface for the growth of a thin film, the requirement of identical films on two different substrates may be hard to satisfy.

2.1.3. Measurement strategy

Let us assume that we can perform the experiment described by Eq. (14) with identical films on different substrates. Then we know the numerical values of the slopes

$$m_1 = K'_{GF} (\alpha_{s1} - \alpha_{f1}) + \alpha_{pf} - \alpha_{f1}, \quad (18)$$

$$m_2 = K'_{GF} (\alpha_{s2} - \alpha_{f1}) + \alpha_{pf} - \alpha_{f1}. \quad (19)$$

Hence, in matrix notation,

$$\begin{pmatrix} 1 & -(1 + K'_{GF}) \\ 1 & -(1 + K'_{GF}) \end{pmatrix} \begin{pmatrix} \alpha_{pf} \\ \alpha_{f1} \end{pmatrix} = \begin{pmatrix} m_1 - K'_{GF} \alpha_{s1} \\ m_2 - K'_{GF} \alpha_{s2} \end{pmatrix}. \quad (20)$$

This system of linear equations is either underdetermined or inconsistent because the determinant of the system matrix vanishes. In the consistent case, i.e., when $m_1 - K'_{GF} \alpha_{s1} = m_2 - K'_{GF} \alpha_{s2}$ or $m_1 - m_2 = K'_{GF} (\alpha_{s1} - \alpha_{s2})$, the equations are solved by infinitely many pairs of parameters $(\alpha_{pf}, \alpha_{f1})$ for given values of K'_{GF} , α_{s1} and α_{s2} . In the inconsistent case $m_1 - m_2 \neq K'_{GF} (\alpha_{s1} - \alpha_{s2})$, which may occur as a result of measurement errors or uncertain parameter values from the literature, the equations do not have a solution at all. Either case is disappointing.

Alternatively, assume that we can perform the experiment described by Eq. (14) with a substrate 1 and, independently, the experiment described by Eq. (8). Then we know the numerical values of the slope m_1 in Eq. (18) and of

$$m_3 = \alpha_{pf} - \alpha_{f1} (= \alpha_R). \quad (21)$$

In matrix notation, Eqs. (18) and (21) can be written as

$$\begin{pmatrix} 1 & -(1 + K'_{GF}) \\ 1 & -1 \end{pmatrix} \begin{pmatrix} \alpha_{pf} \\ \alpha_{f1} \end{pmatrix} = \begin{pmatrix} m_1 - K'_{GF} \alpha_{s1} \\ m_3 \end{pmatrix}. \quad (22)$$

The determinant of the system matrix now is K'_{GF} , i.e., it does not vanish. Therefore, the system of equations has a unique solution. When α_{s1} and K'_{GF} are known, we obtain the following solution for the thin-film parameters:

$$\alpha_{pf} = \alpha_{s1} - \frac{1}{K'_{GF}} m_1 + \left(1 + \frac{1}{K'_{GF}}\right) m_3; \quad (23a)$$

$$\alpha_{f1} = \alpha_{s1} - \frac{1}{K'_{GF}} m_1 + \frac{1}{K'_{GF}} m_3. \quad (23b)$$

When K'_{GF} is not known a priori, but the experiment described by Eq. (14) can be repeated with a different substrate 2, we have Eqs. (18), (19) and (21) at our disposal. By Eq. (17), we can now determine $K'_{\text{GF}} = (m_1 - m_2) / (\alpha_{s1} - \alpha_{s2})$ and eliminate K'_{GF} from Eqs. (23a), (23b). The result is:

$$\alpha_{pf} = \frac{m_2 - m_3}{m_2 - m_1} \alpha_{s1} + \frac{m_1 - m_3}{m_1 - m_2} \alpha_{s2} + m_3; \quad (24a)$$

$$\alpha_{sf} = \frac{m_2 - m_3}{m_2 - m_1} \alpha_{s1} + \frac{m_1 - m_3}{m_1 - m_2} \alpha_{s2}. \quad (24b)$$

It requires two straining experiments and one thermal experiment to uniquely determine the thin-film coefficients α_{pf} , α_{sf} ; and, in addition, the thermal expansion coefficients α_{si} of two substrates must be known. Note that this procedure yields the purely mechanical quantity K'_{GF} , which directly depends on elasticity and piezoresistivity but not on temperature, by way of thermal experiments as the biaxial thin-film strain is realized as thermal-misfit strain.

2.2. Van-der-Pauw experiments

The van-der-Pauw (vdP) theorem applies to geometries involving planar films or plates with arbitrary perimeters, uniform thickness and four contacts A, B, C, D on the periphery (Fig. 1). The current density in such geometries is clearly inhomogeneous. The theorem, derived by conformal mapping methods, relates the resistance $R_{AB, CD}$ measured between terminals C and D when a current is impressed between terminals A and B and the resistance $R_{BC, DA}$ measured between terminals D and A when a current is impressed between terminals B and C [16].

The quantitative statement of the vdP theorem is:

$$\exp\left(-\frac{\pi h}{\rho_f} R_{AB, CD}\right) + \exp\left(-\frac{\pi h}{\rho_f} R_{BC, DA}\right) = 1. \quad (25)$$

Here, h denotes the film thickness and ρ_f is the resistivity of the film material. For symmetric structures with $R_{AB, CD} = R_{BC, DA} = :R$, the theorem reduces to

$$2\exp\left(-\frac{\pi h}{\rho_f} R\right) = 1 \quad (26)$$

or

$$R = \frac{\ln 2 \rho_f}{\pi h}. \quad (27)$$

The resistance varies, when the quantities on the right-hand side vary. Along the same line of reasoning as used in SubSection 2.1, we conclude that

$$\frac{\Delta R}{R} = \frac{\Delta \rho_f}{\rho_f} - \frac{\Delta h}{h} = \frac{\Delta \rho_f}{\rho_f} - \varepsilon_{sf}. \quad (28)$$

As in SubSection 2.1.2, we investigate the effects of thermal expansion only. They are associated with biaxial stress, and Eqs. (2), (9), (10) and (13) hold as before. This also means that Eq. (14) holds as before. As a result, the experiment directly yields the temperature coefficient of

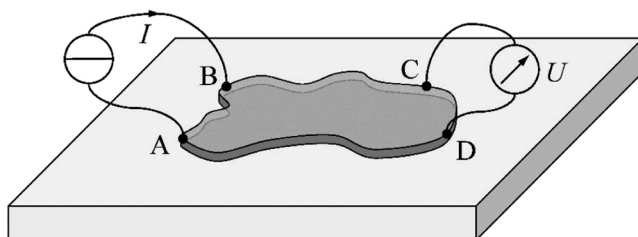


Fig. 1. Test geometry in a vdP experiment.

resistance, α_R , but not the temperature coefficient of the film resistivity, α_{pf} , unless one knows the respective thermal expansion coefficients of the film and the substrate, α_{sf} and α_{s2} , and the effective gauge factor K'_{GF} .

3. Results of application to experimental data

3.1. Geometries with homogeneous current densities

3.1.1. Case 1: 10-nm Au films on glass or polyimide

One finds models other than Eq. (14) in the literature. For example, Oliva et al. propose to use Eq. (14) with K'_{GF} replaced by K_{GF} [17]. This neglects both the transverse piezoresistive effect and the effect of thermal expansion in the thickness direction of the film.

In [17], Eq. (20) is solved with K'_{GF} replaced by K_{GF} and with $\alpha_R = \alpha_{pf} - \alpha_{sf}$ and α_{sf} as unknowns. But rewriting Eq. (20) in the form

$$\begin{pmatrix} 1 & -K_{\text{GF}} \\ 1 & -K_{\text{GF}} \end{pmatrix} \begin{pmatrix} \alpha_R \\ \alpha_{sf} \end{pmatrix} = \begin{pmatrix} m_1 - K_{\text{GF}} \alpha_{s1} \\ m_2 - K_{\text{GF}} \alpha_{s2} \end{pmatrix} \quad (29)$$

does not eliminate the fact that the system determinant vanishes. The system of equations remains underdetermined or inconsistent. We could not gather from [17] how the issue was resolved. In the case of a 10-nm thick gold film deposited at a rate of 0.015 nm/s on borosilicate glass (Corning® Gorilla®) on the one hand and on polyimide (DuPont™ Kapton®) on the other hand, experiments and datasheets provided the data listed in Table 1. This amounts to the inconsistent case as $m_1 - m_2 = 450 \text{ ppm/}^{\circ}\text{C} \neq K_{\text{GF}}(\alpha_{s1} - \alpha_{s2}) = -46.2 \text{ ppm/}^{\circ}\text{C}$.

As expected, the alleged solution $\alpha_R = 894 \text{ ppm/}^{\circ}\text{C}$, $\alpha_{sf} = 67.3 \text{ ppm/}^{\circ}\text{C}$ solves the second row of Eq. (29), up to numerical errors, but not the first one: the left-hand side computes to

$$\begin{pmatrix} 1 & -4.2 \\ 1 & -4.2 \end{pmatrix} \begin{pmatrix} 894 \\ 67.3 \end{pmatrix} \text{ ppm/}^{\circ}\text{C} = \begin{pmatrix} 611.34 \\ 611.34 \end{pmatrix} \text{ ppm/}^{\circ}\text{C}$$

whereas the numbers for the right-hand side are

$$\begin{pmatrix} 1140 - 4.2 \times 9 \\ 690 - 4.2 \times 20 \end{pmatrix} \text{ ppm/}^{\circ}\text{C} = \begin{pmatrix} 1102.2 \\ 606 \end{pmatrix} \text{ ppm/}^{\circ}\text{C}.$$

These expressions deviate too much to suggest an explanation by measurement noise only. It appears as if the observed inconsistency cannot be removed. Neither replacing K_{GF} by the value of K'_{GF} valid without transverse piezoresistivity ($\pi_{xyf} = 0$) nor the value valid in the isotropic case ($\pi_{xyf} = \pi_{xzf}$) do the job. Indeed, to make Eq. (29) consistent would require a gauge factor of

$$K'_{\text{GF, cons}} = \frac{m_1 - m_2}{\alpha_{s1} - \alpha_{s2}} = \frac{450 \text{ ppm/}^{\circ}\text{C}}{(9 - 20) \text{ ppm/}^{\circ}\text{C}} = -40.9,$$

which is not convincing. But this is of only secondary importance. Even if Eq. (29) were consistent with the actual numbers, we would not be able to extract α_R and α_{sf} as infinitely many other data pairs would solve the equation just as well. Our main point is that the entire approach is not applicable without additional equations.

3.1.2. Case 2: 100-nm Au films on glass or polyimide

One starting point to work with additional equations is Eq. (22). Oliva et al. [17] use it with K'_{GF} replaced by K_{GF} and with $\alpha_R = \alpha_{pf} - \alpha_{sf}$ and α_{sf} as unknowns:

$$\begin{pmatrix} 1 & -K_{\text{GF}} \\ 1 & 0 \end{pmatrix} \begin{pmatrix} \alpha_R \\ \alpha_{sf} \end{pmatrix} = \begin{pmatrix} m_1 - K_{\text{GF}} \alpha_{s1} \\ m_3 \end{pmatrix}. \quad (30)$$

The second row immediately yields $\alpha_R = m_3$, which we already know, cf. Eq. (21). In the case of a 100-nm thick gold film deposited at a rate of 0.21 nm/s on the same substrates as in SubSection 3.1.1, experiments and datasheets provided the data listed in Table 2.

The numbers look inconspicuous and we would infer a temperature

Table 1

Data for supported thin gold films from [17].

Substrate No. <i>i</i>	Material	Thin film	m_i (ppm/°C) [17, Tbl. 4]	K_{GF} [17, Fig. 4a]	α_{s1} (ppm/°C) [17, Tbl. 1]	α_R (ppm/°C) [17, Tbl. 5]	α_{f1} (ppm/°C) [17, Tbl. 5]
1	Glass	Au (10 nm), deposited at 0.015 nm/s	1140	4.2	9	894	67.3
2	Polyimide		690		20		

Table 2

Data for supported thin gold films from [17].

Substrate No. <i>i</i>	Material	Thin film	m_i (ppm/°C) [17, Tbl. 2]	K_{GF} [17, Fig. 2 Fig. 2]	α_{s1} (ppm/°C) [17, Tbl. 1]	$m_3 = \alpha_R$ (ppm/°C) [17, Tbl. 3]	α_{f1} (ppm/°C) [17, Tbl. 3]
1	Glass	Au (100 nm), deposited at 0.21 nm/s	3280	8.8	9	3210	17.3
2	Polyimide		3230		20		

coefficient of resistivity of $\alpha_{pf} = \alpha_R + \alpha_{f1} = 3227.3$ ppm/°C for the 100-nm thick gold films. Yet we cannot trust these numbers because, by Eq. (17), we would obtain an effective gauge factor of

$$K_{GF} = \frac{\Delta \alpha'_R}{\Delta \alpha_{s1}} = \frac{m_1 - m_2}{\alpha_{s1} - \alpha_{s2}} = \frac{(3280 - 3230) \text{ ppm/}^\circ\text{C}}{(9 - 20) \text{ ppm/}^\circ\text{C}} \cong -4.54.$$

This is not convincing at all and is likely due to measurement errors. Oliva et al. give a standard uncertainty of $u_m = 130$ ppm/°C for the slopes m_1 through m_3 [17, Tbl. 2 and Tbl. 3]. Error propagation by the usual rules of the Guide to the Expression of Uncertainty in Measurement (GUM) [18–20] then leads to a standard uncertainty of

$$u_{K_{GF}} = \sqrt{\sum_{i=1}^3 \left(\frac{\partial K_{GF}}{\partial m_i} \right)^2 u_m^2} = \frac{\sqrt{2} \cdot u_m}{|\alpha_{s1} - \alpha_{s2}|} \cong 16.7 \text{ (!)}$$

for the effective gauge factor. In other words, the measurement noise does not allow us to estimate K_{GF} in any meaningful manner. The goodness of the result for K_{GF} hinges on (a) the uncertainty u_m of the measured slopes—it should be an order of magnitude smaller than was the case in [17]—and (b) the difference $\alpha_{s1} - \alpha_{s2}$ of the thermal expansion coefficients of the substrates—it should be as large as possible, maybe larger than was the case in [17]. We reiterate that it is not a matter of course to obtain identical thin films on two different substrates.

It is interesting to check if the large uncertainty of the gauge factor K_{GF} also translates into a large uncertainty of the thermal expansion coefficient α_{f1} of a thin film. After all, Eq. (24b) does not contain K_{GF} anymore. Using Eq. (24b) with the numbers from Table 2 yields $\alpha_{f1} \cong 24.4$ ppm/°C for the 100-nm thick gold film. By the law of propagation of random errors [18–20], the standard uncertainty of α_{f1} is

$$u_{\alpha_{f1}} = \sqrt{\sum_{i=1}^3 \left(\frac{\partial \alpha_{f1}}{\partial m_i} \right)^2 u_m^2} = \frac{|\alpha_{s1} - \alpha_{s2}| \cdot u_m}{(m_1 - m_2)^2} \sqrt{(m_1 - m_2)^2 + (m_1 - m_3)^2 + (m_2 - m_3)^2} \quad (31)$$

or, in numbers, $u_{\alpha_{f1}} \cong 50.5$ ppm/°C. The result of $\alpha_{f1} = (24.4 \pm 50.5)$ ppm/°C is of equally doubtful usefulness as the result for K_{GF} . And it differs quite a bit from $\alpha_{f1} = (17.3 \pm 0.3)$ ppm/°C as given in [17, Tbl. 3].

For metal films thicker than about 10 % of the mean free path length of electrons, the Fuchs-Sondheimer theory links the resistivity of a thin film and its thermal coefficient to the corresponding bulk values by [21]

$$\rho_f \alpha_{pf} = \rho_{\text{bulk}} \alpha_{\rho, \text{bulk}}. \quad (32)$$

For gold $\rho_{\text{bulk}} \cong 20.5 \cdot 10^{-9} \Omega \text{m}$ and $\alpha_{\rho, \text{bulk}} \cong 3400$ ppm/°C [17, Tbl. 1]. Hence, with $\alpha_{pf} \cong 3227.3$ ppm/°C as found above, we obtain

$$\rho_f = \frac{\alpha_{\rho, \text{bulk}}}{\alpha_{pf}} \rho_{\text{bulk}} \cong \frac{3400}{3227.3} 20.5 \cdot 10^{-9} \Omega \text{m} \cong 21.6 \cdot 10^{-9} \Omega \text{m}. \quad (33)$$

This result, close to the bulk value, is inconspicuous and would not lead us to suspect any difficulties with the measurement. But what is true for the first-order parameter ρ_f need not be true for the second-order parameter α_{pf} , as we have seen above.

3.1.3. Case 3: 200-nm films of interpenetrating polymer networks on glass

Ziemer et al. [22] prepared and characterized thin films of interpenetrating polymer networks on soda lime glass. The film thickness amounted to about $h = 200$ nm. The authors measured the temperature coefficient of the resistance, α'_R , of various samples and used this as an approximation to the temperature coefficient of the thin-film resistance, α_{pf} . We would like to check if this approximation is justified or not.

The thermal expansion coefficient of soda lime glass ($\text{SiO}_2\text{-Na}_2\text{O}$) depends somewhat on the Na_2O content [3,23, Tbl. 118, Sheets 8–11]. The molar content is likely to be between 10 and 20 % in glasses used as microscope slides, for which case we may assume $\alpha_{s1} \cong 10$ ppm/°C at room temperature [3, Tbl. 118, Sheet 8; 23].

Most pure polymers have $\alpha_{f1} = 10\text{--}60$ ppm/°C [24]. For interpenetrating polymer networks, this, of course, may be different. The same range covers the values for the common photoresist SU-8, be it pure or heavily reinforced and modified by MEMS technology [25]. Without additional knowledge, let us assume $\alpha_{f1} = 30$ ppm/°C as a first guess.

By Eq. (14) and for isotropy ($K_{GF} = 2K_{GF} - 2 - 2\mu_f$):

$$\alpha'_R = 2(K_{GF} - 1 - \mu_f)(\alpha_{s1} - \alpha_{f1}) + \alpha_{pf} - \alpha_{f1}. \quad (34)$$

As $\alpha_{s1} \cong \frac{1}{3} \alpha_{f1}$ with the numbers given above, we can rewrite this in the form

$$\alpha'_R \cong -\frac{1}{3} (4K_{GF} - 1 - 4\mu_f) \alpha_{f1} + \alpha_{pf}. \quad (35)$$

Poisson's ratio for most polymers is in the range $\mu_f = 0.3\text{--}0.4$ [26, p. A10], so we may use the approximate value $\mu_f \cong 0.35$. Neglecting piezoresistivity, about which we know nothing in the case considered, we obtain the purely geometrical estimate $K_{GF} = 1 + 2\mu_f \cong 1.7$. Hence,

$$\alpha'_R \cong -\frac{4.4}{3} \alpha_{f1} + \alpha_{pf} \cong -\frac{4.4}{3} \frac{30 \text{ ppm}}{^\circ\text{C}} + \alpha_{pf} = -44 \text{ ppm/}^\circ\text{C} + \alpha_{pf}. \quad (36)$$

With $\alpha'_R \cong -1.5$ ppm/°C as measured by Ziemer et al. [22], we would conclude that

$$\alpha_{pf} \cong 42.5 \text{ ppm/}^\circ\text{C}. \quad (37)$$

In this case, the true material property α_{pf} turns out to be almost

thirty times greater by magnitude than the estimate one obtains by simply equating α_{pf} with the component property α'_R . In addition, the sign of the estimate is wrong.

As the parameters used in our calculation are uncertain, it is worthwhile to determine the values of α_{pf} which are compatible with the measured value of α'_R and the possible ranges of the parameters. The most uncertain parameters are α_{rf} and K_{GF} . As mentioned above, we may assume $\alpha_{rf} = 10\text{--}60 \text{ ppm/}^\circ\text{C}$. The gauge factor K_{GF} ranges from values below 1 to >100 . The largest values are observed in polymer-

filler composites—think of carbon nanotubes in homogenous polymer substrates—with filler contents just below the percolation threshold [27]. In most cases, however, and at the low strains applied by Ziemer et al. [22], $K_{GF} = 0.5\text{--}10$ [28,29]. Unfortunately, the intervals $\alpha_{rf} = 10\text{--}60 \text{ ppm/}^\circ\text{C}$ and $K_{GF} = 0.5\text{--}10$ lead to permissible values of α_{pf} between $-175 \text{ ppm/}^\circ\text{C}$ and $925 \text{ ppm/}^\circ\text{C}$ (Fig. 2a). In other words: almost nothing can be said about α_{pf} unless α_{rf} and K_{GF} can be restricted to smaller intervals or are even known by independent measurements. For example, should we know $\alpha_{rf} = (30 \pm 5) \text{ ppm/}^\circ\text{C}$ and $K_{GF} = 2 \pm$

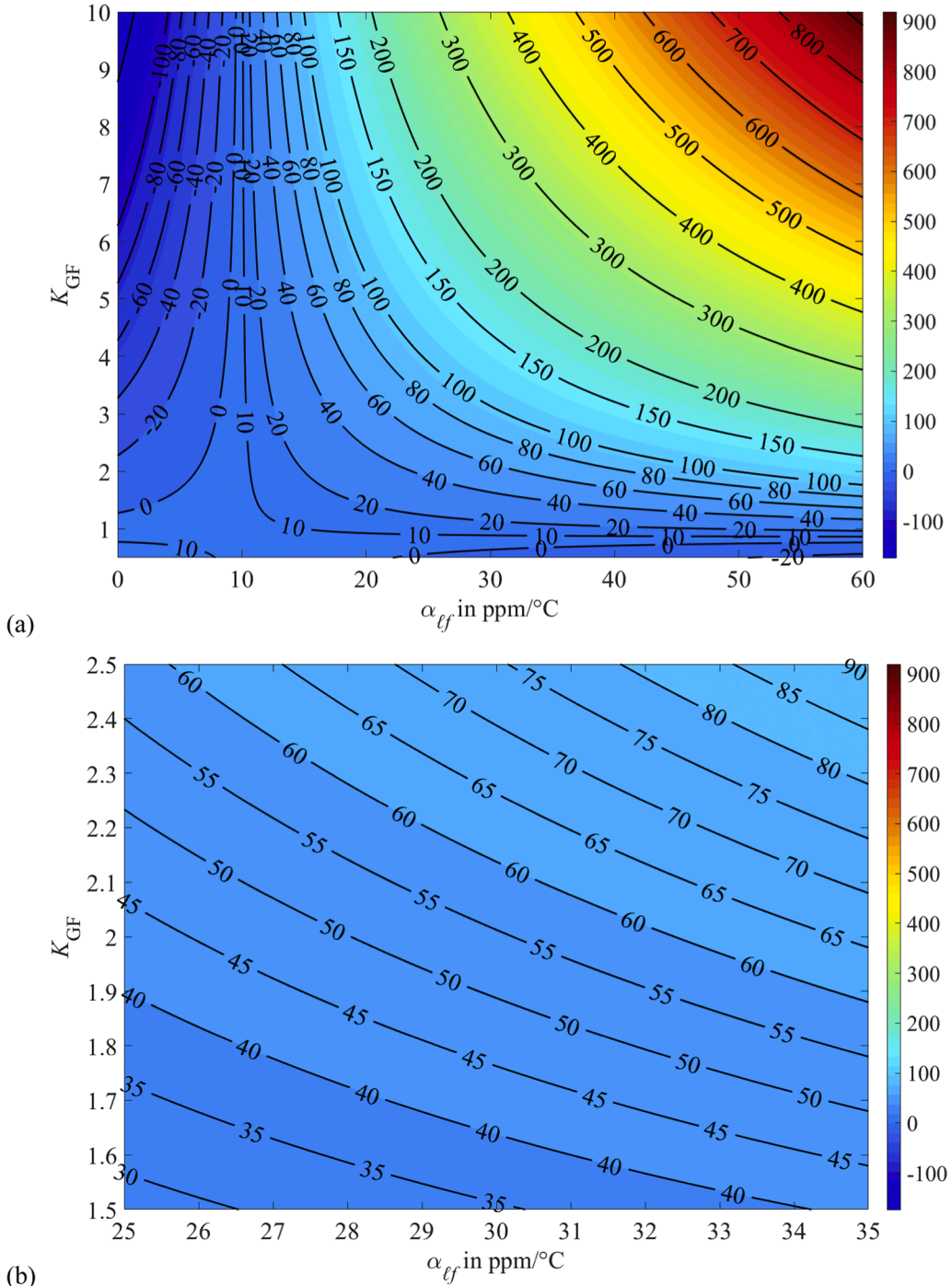


Fig. 2. Temperature coefficient of resistivity, α_{pf} , of a thin film of an interpenetrating polymer network on soda lime glass derivable by Eq. (34) from the measured temperature coefficient of the resistance, α'_R , as a function of the gauge factor K_{GF} and the coefficient of thermal expansion α_{rf} . As the latter two parameters are unknown, plausible intervals for their values have been assumed. (a) Overview image for large interval range (assuming maximum uncertainty of K_{GF} and α_{rf}). (b) Close-up for restricted interval range.

0.5, then we can pinpoint α_{pf} to a value of (60 ± 30) ppm/ $^{\circ}\text{C}$ (Fig. 2b). This is still not an extremely pleasing result, but it is better than no knowledge at all and in any case it reflects the often overlooked fact that α_{pf} is hard to determine.

3.2. Van-der-Pauw experiments

The influence of α_{sf} , let alone α_{ss} and K'_{GF} , is sometimes neglected in the literature without proper justification. For example, Pal et al. [30, 31] use the vdp method to infer the temperature-dependent resistivity of thin-film materials from resistances measured at various temperatures and from *room-temperature* film thicknesses. This amounts to neglecting the influence of α_{sf} .

The literature cites a bulk value of $\alpha_{sf} = 13$ ppm/ $^{\circ}\text{C}$ for the thermal expansion coefficient of cobalt at room temperature [32, p. 70; 33, p. 12-216]. Assuming this value to also hold for the cobalt thin films of [30] gives the following correction for a 100-nm cobalt film deposited at 150 $^{\circ}\text{C}$ on a glass substrate [30, fig. 6]:

$$\alpha_{pf} \cong 700 \text{ ppm}/^{\circ}\text{C} \rightarrow \alpha_{pf} \cong 713 \text{ ppm}/^{\circ}\text{C}. \quad (38)$$

Likewise, for a 100-nm tin film ($\alpha_{sf} = 22$ ppm/ $^{\circ}\text{C}$ at room temperature [32, p. 339; 33, p. 12-217] deposited on glass [31, Fig. 2Fig. 2]:

$$\alpha_{pf} \cong 3400 \text{ ppm}/^{\circ}\text{C} \rightarrow \alpha_{pf} \cong 3422 \text{ ppm}/^{\circ}\text{C}. \quad (39)$$

In this case the errors are not large, $13/700 \cong 1.9\%$ and $22/3400 \cong 0.6\%$, and may be neglected. This should not tempt one to take such luck for granted in other cases. To be on the safe side, it is preferable to avoid conceptual errors from the outset.

4. Discussion

In most cases, it is not possible to investigate suspended thin films. Nor does it make sense, as thin films are normally supported by a substrate in practical applications. Our analysis of such supported films has shown

- (1) that it requires two straining experiments and one thermal experiment to uniquely determine the thin-film coefficients α_{sf} (temperature coefficient of resistivity) and α_{sf} (thermal expansion coefficient) and
- (2) that, in addition, the thermal expansion coefficients α_{si} of two substrates must be known and
- (3) that, finally, one must be able to deposit identical copies of a thin film on the two substrates.

As a cursory glance at the literature shows, quite a few reports approximate α_{pf} , a material property, by the measured coefficient of resistance α'_R of a supported thin-film resistor, a device property. Our re-evaluation of some cases has shown how poor this approximation can be. And even when researchers are aware of the difference between α_{pf} and α'_R , the complexity of the situation and experimental difficulties can lead and have led to incorrect conclusions in that the material parameters determined satisfy one but not all of the required equations (inconsistent case) or represent only one of infinitely many equally valid solutions (underdetermined case).

We believe that our framework in the first place and the demonstration of the use of uncertainty measures according to GUM—practically absent from the literature on thin-film measurements to date—in the second place can help avoid similar pitfalls in the future.

5. Conclusions

It is generally known that the effective material properties of thin films may deviate from the corresponding bulk values. This understanding has spawned and continues to spawn much experimental work

dedicated to directly measuring the material properties of thin films. As we have shown, it requires two substrates, two straining experiments, one thermal experiment, and the knowledge of the thermal expansion coefficients α_{si} of the two substrates to uniquely determine the thin-film temperature coefficient of resistivity by Eqs. (24a, 24b). As we have shown by way of examples, it is easy to overlook one or more of these conditions and experimental difficulties can lead to large uncertainties. In any case, the allegedly measured value of the temperature coefficient of resistivity may violate necessary requirements (and thus simply be wrong) or be an arbitrary pick from an infinite set of valid solutions.

In case of doubt, it is advisable not to specify the temperature coefficient of resistivity α_{pf} of a thin film, but only the measured temperature coefficient of resistance α'_R . Although the latter is a device property and thus involves both material properties and geometry details, correct knowledge of its temperature behavior is preferable to incorrect knowledge of the temperature behavior of the resistivity.

CRediT authorship contribution statement

Gerhard Fischerauer: Writing – review & editing, Writing – original draft, Visualization, Validation, Supervision, Software, Methodology, Investigation, Formal analysis, Conceptualization.

Declaration of competing interest

The authors declare that they have no known competing financial interests or personal relationships that could have appeared to influence the work reported in this paper.

Data availability

The data used in the article are accessible in the published literature.

References

- [1] F.S. Hickernell, T.S. Hickernell, M. Liaw, The acoustic properties of PECVD thin-film silicon-carbide, in: Proc. Ultrason. Symp., Baltimore, MD, 1993, pp. 273–275, <https://doi.org/10.1109/ULTSYM.1993.339573>. Oct. 31 – Nov. 3.
- [2] F.S. Hickernell, T.S. Hickernell, Surface acoustic wave characterization of PECVD films on gallium arsenide, IEEE Trans. Ultrason., Ferroelectr., Freq. Control 42 (1995) 410–415, <https://doi.org/10.1109/58.384451>.
- [3] J.F. Shackelford, W. Alexander, Materials Science and Engineering Handbook, 3rd ed., CRC Press, Boca Raton etc, 2001.
- [4] B.K. Sharma, R. Srivastava, Negative temperature coefficient of resistivity of thin metallic wires, J. Mat. Sci. Lett. 2 (1983) 775–776, <https://doi.org/10.1007/BF00720557>.
- [5] E.H. Sondheimer, The mean free path of electrons in metals, Adv. Phys. 1 (1952) 1–42, <https://doi.org/10.1080/00018735200101151>.
- [6] A.F. Mayadas, M. Shatzkes, Electrical-resistivity model for polycrystalline films: the case of arbitrary reflection at external surfaces, Phys. Rev. B 1 (1970) 1382–1389, <https://doi.org/10.1103/PhysRevB.1.1382>.
- [7] E.E. Mola, J.M. Heras, Exact and approximate equations for the thickness dependence of resistivity and its temperature coefficient in thin polycrystalline metal films, Thin Solid Films 18 (1973) 137–144, [https://doi.org/10.1016/0040-6090\(73\)90231-9](https://doi.org/10.1016/0040-6090(73)90231-9).
- [8] J.R. Sambles, The resistivity of thin metal films—Some critical remarks, Thin Solid Films 106 (1983) 321–331, [https://doi.org/10.1016/0040-6090\(87\)90086-1](https://doi.org/10.1016/0040-6090(87)90086-1).
- [9] J.B. Thompson, The resistivity, temperature coefficient of resistivity and thermoelectric power of thin continuous metal films I: a survey and critical appraisal of the application of processing methods to experimental data, Thin Solid Films 150 (1987) 145–162, [https://doi.org/10.1016/0040-6090\(87\)90086-1](https://doi.org/10.1016/0040-6090(87)90086-1).
- [10] J.B. Thompson, The resistivity, temperature coefficient of resistivity and thermoelectric power of thin continuous metal films II: a methodology for computer-processing of thin-film data to extract parameters with associated error-estimates, Thin Solid Films 150 (1987) 163–174, [https://doi.org/10.1016/0040-6090\(87\)90087-3](https://doi.org/10.1016/0040-6090(87)90087-3).
- [11] B. Morten, L. Pirozzi, M. Prudenzati, A. Taroni, Strain sensitivity in film and cermet resistors: measured and physical quantities, J. Phys. D: Appl. Phys. 12 (1979) L51–L54, <https://doi.org/10.1088/0022-3727/12/5/003>.
- [12] M.S. Zarnik, D. Belavić, A. Wymyslowski, Evaluation of gauge coefficients for modelling piezoresistive properties of thick-film resistors, Sensor. Mater. 18 (2006) 261–275.
- [13] A. Müller, M.C. Wapler, U. Wallrabe, A quick and accurate method to determine the Poisson's ratio and the coefficient of thermal expansion of PDMS, Soft Matter 15 (2019) 779–784, <https://doi.org/10.1039/c8sm02105h>.

[14] Ch.-Ch. Chiu, Determination of the elastic modulus and residual stresses in ceramic coatings using a strain gage, *J. Am. Ceram. Soc.* 73 (1990) 1999–2005, <https://doi.org/10.1111/j.1151-2916.1990.tb05258.x>.

[15] Z. Rosenberg, On the elastic strain coefficients of the resistance of metals, *Mater. Sci. Eng.* 100 (1988) L9–L10, [https://doi.org/10.1016/0025-5416\(88\)90268-6](https://doi.org/10.1016/0025-5416(88)90268-6).

[16] L.J. van der Pauw, A method of measuring specific resistivity and Hall effect of discs of arbitrary shape, *Philips Res. Rep.* 13 (1958) 1–9.

[17] A.I. Oliva, J.M. Lugo, R.A. Gurubel-Gonzalez, R.J. Centeno, J.E. Corona, F. Aviles, Temperature coefficient of resistance and thermal expansion coefficient of 10-nm thick gold films, *Thin Solid Films* 623 (2017) 84–89, <https://doi.org/10.1016/j.tsf.2016.12.028>.

[18] L. Kirkup, R.B. Frenkel, *An Introduction to Uncertainty in Measurement Using the GUM (Guide to the Expression of Uncertainty in Measurement)*, Cambridge University Press, Cambridge, 2006.

[19] JCGM 100:2008, GUM 1995 with minor corrections: evaluation of measurement data—guide to the expression of uncertainty in measurement, Joint Committee for Guides in Metrology, s.l. (2008).

[20] ISO/IEC Guide 98-3:2008, *Uncertainty of Measurement—Part 3: Guide to the Expression of Uncertainty in Measurement*, ISO, Geneva, Switzerland, 2008.

[21] S.E. Gustafsson, E. Karawacki, M.N. Khan, Simultaneous measurement of resistivity and temperature coefficient of resistivity of metallic thin films with the transient hot-strip method, *Thin Solid Films* 92 (1982) 287–294, [https://doi.org/10.1016/0040-6090\(82\)90011-6](https://doi.org/10.1016/0040-6090(82)90011-6).

[22] T. Ziemer, G. Ziegmann, C. Rembe, Investigation of the properties of electrically conductive interpenetrating polymer networks for the use as temperature sensors, *TM-Tech, Meas* 89 (2022) S8–S13, <https://doi.org/10.1515/teme-2022-0066>.

[23] Data Sheet, Precision Cover Glasses and Microscope Slides, Thorlabs Inc. Available online: https://www.thorlabs.de/newgroupage9.cfm?objectgroup_id=9704 (accessed on Apr. 15, 2024).

[24] N. Kinjo, M. Ogata, S. Numata, Thermal expansion coefficients of polymers (in Japanese), *J-Stage* 8 (1987) 208–221, <https://doi.org/10.11364/networkpolymer1980.8.208>.

[25] W. Zhou, Y. Li, Y. Sun, J. Yao, X. Song, G. Ding, Enhancement of mechanical and thermal properties of SU-8 photoresist with multilayer woven glass fabric based on micromachining technology, *Electron. Mat. Lett.* 16 (2020) 604–614, <https://doi.org/10.1007/s13391-020-00247-8>.

[26] W.D. Callister Jr., *Materials Science and Engineering*, 7th ed., John Wiley & Sons, New York, 2007.

[27] K. Ke, V. Solouki Bonab, D. Yuan, I. Manas-Zloczower, Piezoresistive thermoplastic polyurethane nanocomposites with carbon nanostructures, *Carbon N Y* 139 (2018) 52–58, <https://doi.org/10.1016/j.carbon.2018.06.037>.

[28] P. Costa, S. Ribeiro, S. Lanceros-Mendez, Mechanical vs. electrical hysteresis of carbon nanotube/styrene-butadiene-styrene composites and their influence in the electromechanical response, *Compos. Sci. Technol.* 109 (2015) 1–5, <https://doi.org/10.1016/j.compscitech.2015.01.006>.

[29] J.R. Diós, C. García-Astrain, S. Gonçalves, P. Costa, S. Lanceros-Méndez, Piezoresistive performance of polymer-based materials as a function of the matrix and nanofiller content to walking detection application, *Compos. Sci. Technol.* 181 (2019) 107678, <https://doi.org/10.1016/j.compscitech.2019.107678>, 1–12.

[30] K. Pal, S. Chaudhuri, A.K. Barua, The electrical resistivity and temperature coefficient of resistivity of cobalt films, *J. Phys. D: Appl. Phys.* 9 (1976) 2261–2267, <https://doi.org/10.1088/0022-3727/9/15/017>.

[31] K. Pal, P. Sen, Resistivity and temperature coefficient of resistivity of tin films, *J. Mat. Sci.* 12 (1977) 1472–1476, <https://doi.org/10.1007/BF00540864>.

[32] Y.S. Touloukian, R.K. Kirby, R.E. Taylor, P.D. Desai, *Thermal Expansion: Metallic Elements and Alloys (= Thermophysical Properties of Matter)*, 12, IFI/Plenum, New York and Washington, 1975.

[33] W.M. Haynes, *CRC Handbook of Chemistry and Physics* (ed), 97th Edition, CRC Press, Boca Raton, Florida, 2017.